ORIGINAL RESEARCH

Biosorption efficacy of alginate-immobilized live and metal chloride-activated *Azolla microphylla* in Pb(II) removal from aqueous solution

Alicia Hui-Ying Khor . Kok-Song Lai . Hon-Jung Liew . Jiun-Yan Loh

Abstract Pb(II) biosorption of untreated (CA-UT), and treated or metal chloride-activated (CA-T) *Azolla microphylla* microencapsulated with calcium alginate were investigated for contact time, pH, and temperature in the present study. Pb(II) biosorption rate was recorded highest within the first hour at pH 4.5-5.0. Albeit, no significant difference at 25 ± 2 °C, and 40 °C. The biosorption kinetics were further described by pseudo-first- and second-order and multi-linear intraparticle diffusion graphs. Results showed that R^2 values was recorded at $0.4619 – 0.9912$ in the pseudo-first-order model, while in the pseudo-second-order model, R^2 values was recorded at $0.9936 – 1.000$. These kinetic models indicated the biosorption process of Pb(II) is a complex mechanism and influenced by various factors predominantly the pH and time of exposure. Maximum lead removal efficiency for metal uptake was recorded at 2 mg of Pb(II) per gram of biosorbent at pH 4.5–5.0 at 25 ± 2 °C, and 40 °C. The Pb(II) biosorption efficiency was generally increased from CA-UT < CA < CA-T. This study demonstrated the applicability and effectiveness of *A. microphylla* in lead abatement, which could be a potential approach in phytoremediation for sewage treatment plant.

Introduction

Over the past centuries, the outgrowth of anthropogenic activities and the inefficient enforcement of environmental regulations in many countries have resulted in inevitable environmental destruction, such as heavy metal pollution (Gebremedhin and Berhanu 2015). Heavy metals are toxic, and they often cause irreversible adverse effects on the ecological chains and its inhabitants (Ali et al. 2019). It is a well-established fact that the toxicity of heavy metals is often associated with the type of metal, exposure rate, and route, as well as the physiology of exposed individuals (Ab Razak et al. 2015). Among the heavy metals, lead (Pb) is of significant concern to the public due to their highly toxic nature, and biomagnification effects in the aquatic environment (Jeyakumar and Chandrasekaran 2014). Studies show that lead metal exposure could disrupt physiological, biochemical, and behavioral functions in aquatic organisms, as well as in humans (Fu and Wang 2011; Sharma et al. 2014).

Alicia Hui-Ying Khor, Jiun-Yan Loh (✉)
Faculty of Applied Sciences, UCSI University. No. 1, Jalan Menara Gading, UCSI Heights, Cheras, 56000, Kuala Lumpur, Malaysia
e-mail: lohjy@ucsiuniversity.edu.my

Kok-Song Lai
Health Sciences Division, Abu Dhabi Women's College, Higher Colleges of Technology, 41012 Abu Dhabi, United Arab Emirates

Hon-Jung Liew
Institute of Tropical Aquaculture and Fisheries (AKUATROP), Universiti Malaysia Terengganu, 21030, Kuala Terengganu

Chemical precipitation, ultrafiltration, and electrochemical treatments are commonly used to mitigate heavy metal pollution in wastewater (Salman et al. 2012). However, they are labor-intensive, require large energy input, and costly in terms of operation. In recent years, biosorption has emerged to be a promising alternative in heavy metal abatement. Biosorption is an environmentally friendly and cost-effective approach that requires lower energy input. It utilizes the metal sequestering properties of natural materials from the biological origin (Hlaing et al. 2011). Among the water plants, *Azolla* has been regarded as an emerging biosorbent for heavy metal due to its unique biosorption capacity associated with the metal-binding on the plant cell walls (Sood et al. 2012).

Azolla is a free-floating aquatic fern member of the Azollaceae family. This plant is native to Asia, Africa, and America. Owing to its N-fixing abilities, quick biomass doubling rate, toleration, and accumulation of a vast range of pollutants, the fern has been explored for various scientific research. The plant can extensively colonize both fresh and contaminated non-turbulent water bodies (Sood et al. 2012). Its invasive nature may be seen as an ecological threat, however, studies showed that this species could be a promising candidate for heavy metal biosorption (Taghi et al. 2005). *Azolla* biosorption capacity is largely attributed to its cell wall polysaccharide constituents, e.g. pectin and cellulose. The carboxyl groups in these constituents react with Ca^{2+} or Mg^{2+}, forming three-dimension polymers, $(-COO)_2Ca$ and $(-COO)_2Mg$, which act as the bases for heavy metal ion exchange. Similar to a study by Raize et al. (2002), lead removal could be activated through sequestration mechanism by the plant biomass, the binding mechanisms included a combination of ion exchange, chelation, and also reduction reactions. When *Azolla* treated with oxidation agents, this could further enhance heavy metal removal ability due to metallic lead precipitation on the plant's cell wall matrix (Raize et al. 2002; Khosravi et al. 2005).

Biosorbent immobilization is a common technique used to increase biosorption potential in industrial applications (Kanamarlapudi et al. 2018). Among these techniques, calcium alginate encapsulation is a common, economic, and simple way to reinforce the durability of bio-matrix. Encapsulation of *Azolla* using calcium alginate is able to reinforce its durability, while facilitating heavy metal separation during wastewater treatment. This study aims to investigate Pb(II) biosorption capacity, biosorption kinetics and biosorption mechanisms of *A. microphylla* encapsulated in calcium alginate. The outcome of the study provides a comprehensive conception of the potential use of phytoremediation in industrial wastewater treatment.

Materials and methods

Azolla biomass preparation

Azolla microphylla was collected from a local harvester (Puchong - Batu Dua Belas, Selangor, Malaysia). Fresh *Azolla* sample (~1kg) was cleaned with 1 L of distilled water to remove debris. The samples were squeezed and dried in the hot air oven at 50 °C for 24 h. After drying, the sample was minced using an electric homogenizer (LabGEN 125, Cole-Parmar, USA), and sieved through a mesh (~1.5 mm) to obtain powder-like particles. The sieved *Azolla* sample (categorized as untreated *Azolla*, UT) was placed in a covered glass beaker for the subsequent experiments. Two different treatments were studied i.e. immobilized dried *Azolla* (CA-UT, untreated and calcium alginate microencapsulated *Azolla*) and the immobilized dried *Azolla* with metal chloride-activated treatment (CA-T, treated and calcium alginate microencapsulated *Azolla*).

Metal chloride-activated treatment of Azolla biomass

All treatment procedures were carried out at room temperature (24 ± 2 °C) and agitation rate at 150 rpm (Shaking incubator; Bibby Scientific™- SI500, Stuart, UK). Dried *Azolla* sample (1 g) was firstly treated with 0.2 M NaOH (1:10 w/v) at pH 10.5 ± 0.2. The sample was then filtered and washed five times with distilled water to remove excess Na^+ ions. Subsequently, the sample was treated with a combination of 1:0.5:0.5 molar ratio of $CaCl_2/MgCl_2/NaCl$, at 1 g sample: 250 mL chloride salts solutions ratio (1:250 w/v) for 5 hours. The sample was then filtered and washed for another five times with distilled water to remove excess cations. Finally, the filtered sample was dried in the hot air oven at 50°C for 20 hours and kept in an airtight container before the microencapsulation (CA-T beads) process (Khosravi et al. 2005).
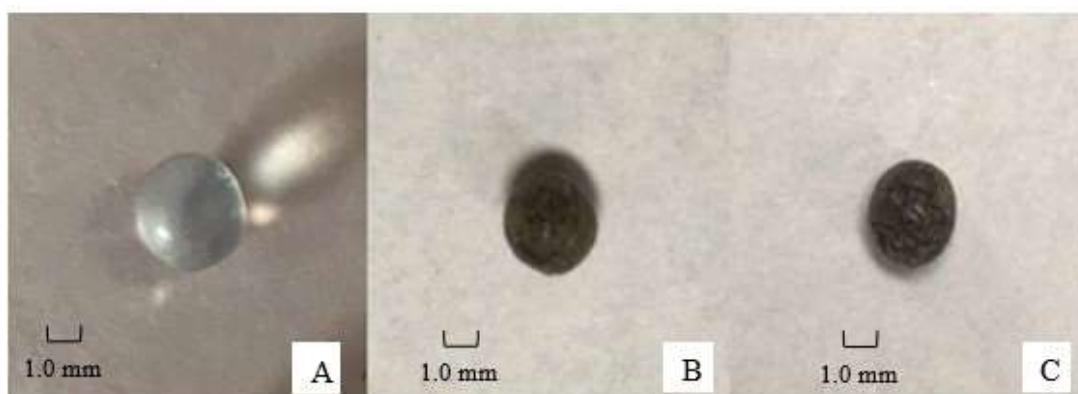
Fig. 1 A. a plain calcium alginate bead (CA), B. untreated *Azolla* alginate bead (CA-UT), and C. treated *Azolla* alginate bead (CA-T). The average diameter of beads ranging at 3.9 ± 0.3 mm^{-1} bead

Preparation of calcium alginate beads

Sodium alginate (Na-Alg) solution 1% (w/v) was prepared by dissolving Na-Alg (R & M Marketing Essex, UK) in distilled water, and left in a refrigerator (at 4°C) for overnight. The alginate microencapsulation experiments were divided into three groups. One group labelled as calcium alginate beads loaded with chloride-activated treated *Azolla* (CA-T), calcium alginate beads loaded with untreated *Azolla* (CA-UT), and control of unloaded calcium alginate beads (without the addition of *Azolla,* CA), respectively. All experiments were performed in triplicates.

The *Azolla* of CA-T and CA-UT were settled in the sodium alginate. A concentration of 1% (w/v) sodium alginate was used to prevent the clogging issue in the 50 mL syringe. The sodium alginate solution containing *Azolla* was mixed evenly and dripped carefully into a 0.2 M $CaCl_2$ solution without agitation (Merck, Germany). The formation of alginate beads was carried out carefully and measured using a caliper to ensure the diameter between beads was at the lowest discrepancy (3.9 ± 0.3 mm) among the treatments. The beads were left in the $CaCl_2$ solution for overnight at 4 °C. The beads were then rinsed with distilled water and stored at 4 °C based on assigned groups (Figure 1) in different Schott bottles before use.

Pb(II) biosorption experimental design

Batch biosorption experiments were conducted to determine Pb(II) removal efficiency in the beads (CA, CA-UT, and CA-T). A 1000 mg L^{-1} lead nitrate stock solution was prepared by dissolving $Pb(NO_3)^2$ (GENE Chem, Canada) in distilled water. The pH of Pb(II) solutions was adjusted with 0.1M HCl (Merck, Germany) or 0.1M NaOH (Merck, Germany), to obtain specific pH values of 4.5, 5.0, 5.5, and 6.0. Biosorption experiments were carried out by adding 1 g of beads into 20 mL of 100 mg L^{-1} lead solution (1:20 w/v) at different pH mentioned earlier. The mixtures were subsequently agitated with a shaking incubator at 150 rpm for 6 hours, at 24 ± 2°C, and 40°C. The samples were analysed at 60, 120, 180, 240, 300, and 360 min intervals using a flame atomic absorption spectrophotometer, AAS (PerkinElmer Analyst 100, air-acetylene flame, 15mA/324.8 nm, USA). The sample analysis was conducted in triplicates, with each replicate was repeated thrice to ensure the consistency of data.

The percentage of Pb(II) adsorbed by the beads in the aqueous solutions were calculated using the following equation:

$$\text{Heavy Metal Removal Efficiency (\%)} = \frac{c_i - c_f}{c_i} \times 100 \qquad \text{(Equation 1)}$$

Where, C_f is the final, and C_i is the initial concentration of heavy metal in aqueous solution (in mg L^{-1}). The assessment on the Pb(II) biosorption efficiency of CA, CA-UT, and CA-T at different pH, i.e. pH 4.5, 5.0, 5.5, and 6.0 was investigated using the same experimental set-up.

Kinetic studies

The amount of Pb(II) adsorbed per unit weight of beads were calculated using the following equation:

$$\text{Heavy Metal Uptake Capacity,} \, q_t \, (mg/g) = \frac{c_i - c_f}{W} V \qquad \text{(Equation 2)}$$

Where, V is the volume of heavy metal solution (L), and W is the mass of beads (g).

The mechanism of Pb(II) biosorption process was determined by the pseudo-first-order equation, pseudo-second-order, and intraparticle diffusion models:

Pseudo-first-order formula (Lagergren 1898):

$$\log(q_e - qt) = \log q_e - \left(\frac{k_1}{2.303}\right) t \qquad \text{(Equation 3)}$$

Pseudo-second-order formula (Ho and McKay 2000):

$$\frac{t}{q_t} = \frac{1}{k_2 q_e^2} + \frac{t}{q_e} \qquad \text{(Equation 4)}$$

Intraparticle diffusion formula (Quiton et al. 2018):

$$q_t = k_p \cdot t^{\frac{1}{2}} + k_d \qquad \text{(Equation 5)}$$

Where q_e and q_t are the amount of Pb(II) ions adsorbed per unit weight of beads at equilibrium and at time t, respectively (mg g^{-1}); k_1 and k_2 is the rate constant of pseudo-first-order biosorption (min^{-1}) and pseudo-second-order biosorption (g mg^{-1} min), respectively; k_d is the boundary resistant constant (mg g^{-1}), and k_p is the intraparticle diffusion rate constant (mg g^{-1} min$^{-1/2}$).

Fourier Transform Infrared spectroscopy (FTIR) characterization

Fourier Transforms Infrared (FTIR) spectroscopy was used to characterize the functional groups responsible for heavy metals biosorption on the biosorbents i.e. CA, CA-UT, and CA-T beads, and the fresh sample of *A. microphylla.* The CA-T, CA-UT, CA, and *Azolla* biomass (prepared as previously mentioned in Azolla biomass preparation) were air-dried at room temperature (25 ± 2 ºC) for 24 hours. The samples were ground into a fine powder and mixed in a potassium bromide, KBr matrix before FTIR analysis. Functional group characterization of the biosorbents was performed using Thermo Scientific Nicolet iS5 FT-IR spectrophotometer (Thermo Fisher, USA), with a scanning range within 4000-400 cm^{-1} in 256 scans at a resolution of 1 cm^{-1}. The analysis was performed in triplicate to ensure data consistency.

Results and discussion
Influence of contact time

The influence of contact time on Pb(II) biosorption under various pH values and temperatures, were investigated in hourly intervals for a period of 360 minutes (Fig. 2). Rapid biosorption occurred within the first 60 minutes, where all samples showed over 70% lead removal efficiency. After the first hour, the biosorption rate dropped, however, lead removal efficiency remained at a steady rate. At 360 minutes, the maximum lead removal efficiencies for CA, CA-UT, and CA-T beads were recorded at 97.47, 96.67, and 97.86%, respectively. CA-T beads showed slightly better lead biosorption compared to CA and CA-UT. A large portion of lead biosorption is due to the use of alginates. Alginate is a strong binder contains carboxyl, amido, hydroxyl, phosphate, and sulfonic groups which can bind to heavy metal ions. The porous structure of alginate also plays a significant role in the absorption process (Zhao et al. 2018). Pre-treatment of *Azolla* with metal-chloride activated preparation in this study suggested the surface characteristics of the cell wall of *Azolla* could have been modified and thus influenced the biosorption process (Mashkani and Ghazvini 2009). Studies showed that biosorption of heavy metals like Cr(VI) and Pb(II) occurs within the first contact hour in the adsorbent, and the trend slows down gradually with prolonged time (Fiol et al.

2005, Naga et al. 2017). Similarly, Uysal and Taner (2009) reported the lead concentrations were decreased rapidly in 24 h when treated with duckweed in an aqueous solution (*Lemna minor*). During 24 to 72 h, the Pb(II) biosorption by *L. minor* remained stable and reached the equilibrium after 360 min, this indicating that the availability of the biosorbent binding has reached to its saturation (Tseveendorj et al. 2018). The biosorption involved in this process indeed a very complex mechanism. The biosorbent e.g. *Azolla* removed lead from aqueous through either the binding of metal ions chemically (ion exchange), or physically (van der Waals forces or the electrostatic interaction between the biosorbent matrix and metals) or via reduction, chelation, complexation and precipitation (Kanamarlapudi et al. 2018).
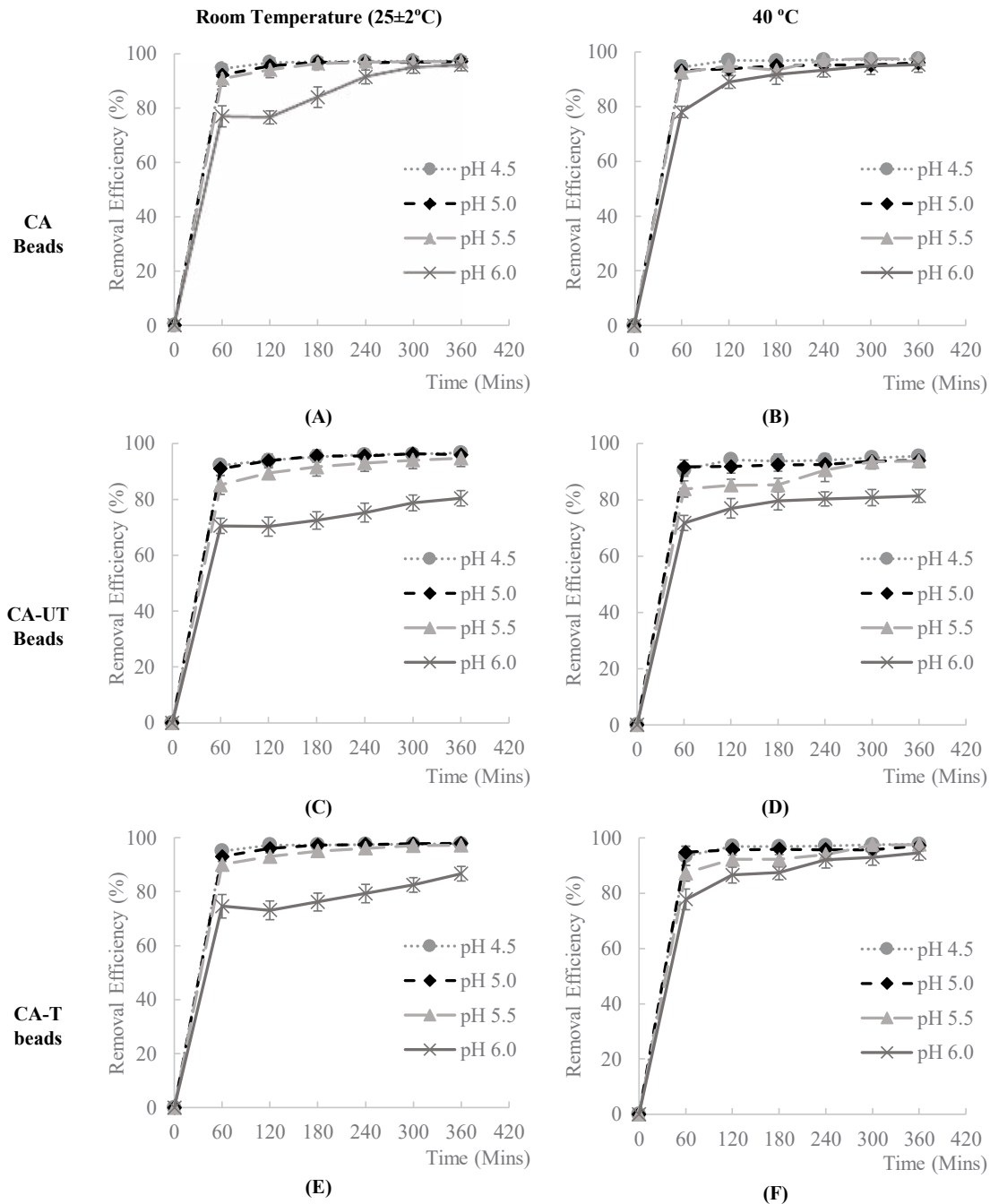

Fig. 2 Removal efficiency (%) against time (min) for (A and B) CA beads, (C and D) CA-UT beads, and (E and F) CA-T beads at room temperature, 25±2 ºC (in A; C; E) and 40 ºC (in B; D; F). Vertical bars indicate standard deviation of means

Influence of pH

Numerous studies indicated that heavy metal biosorption is strongly influenced by pH (Salman et al. 2014). It is well known that pH value is an important parameter for heavy metal biosorption processes, it influences metal-biosorbent interaction, the solubility of metal ions, and the charge of functional groups on biosorbents (Wei et al. 2016). In this study, pH influential on Pb(II) biosorption was examined at different pH values (4.5 – 6.0). The experiment was not performed at pH > 6.0, as high pH causes high precipitation of lead in the solution (Kariuki et al. 2017). Our present results showed that maximum lead biosorption for CA beads was reached to 97.47% (pH 5.5) followed by CA-UT at 96.67% (pH 4.5), and CA-T at 97.86% (pH 5.0), respectively.

Figure 2 showed a minor difference in lead removal efficiency between CA-UT and CA at pH 4.5 – 5.5 at room temperature. Likewise, lead removal efficiency also observed in minor changes in the treatment of CA-UT and CA-T both treated at 40°C under pH in the range of 4.5 – 5.0. In terms of temperature, the lead removal efficiency is consistent among the pH with an exceptional case in pH 6.0, whereby noticeable inconsistency was observed in the groups of CA and CA-T. Despite this, the removal efficiency rate dropped slightly at pH of 5.5 in CA-UT and CA-T. The treatment groups still exhibited high removal efficiency, i.e. 94.73% for CA-UT and 97.55% for CA-T, respectively at 360 minutes. Above pH 5.5, Pb(II) removal efficiency dropped drastically (i.e. 80.41 – 95.8%), regardless of bead type and temperature. The decrease in removal efficiency under pH 6.0 may be attributed to the increases of PbO_2^{2-} (Plumbate) anions and decreased of Pb^{2+} cations in the aqueous solutions. This is in agreement with Uysal and Taner (2009), the authors claimed that highest accumulated lead concentration at 3.599 mg Pb g^{-1} was found in *L. minor* at pH 4.5, and the lead accumulation dropped as the pH increased to pH 6.0 and above.

Some studies demonstrated that pH 4.5 (Sanyahumbi et al. 1998) and 5.0 (Taghi et al. 2005) are the optimal pHs in lead biosorption using *Azolla* sp. as a biosorbent. While using calcium alginate as a sole biosorbent has optimal biosorption at slightly higher pH compared to *Azolla* i.e. pH 5.0 (Hlaing et al. 2011) and 6.0 (Naga Babu et al. 2017). The present study showed that *Azolla*-biosorbent can effectively remove lead from the aqueous at pH 4.5 – 5.5.

In common cases, heavy metal absorption is correlated with pH value. This mainly due to the increasing concentration of protons (H^+). Ions hydrogen (H^+) are tended to bind on the biosorbent's surface as compared to Pb^{2+} (Rahman and Sathasivam 2015). In an acidic addition, low pH promotes protonation of sequestering groups on the biosorbent's surface by altering its charges. This resulting in a repulsive force between the adsorbent surface and Pb^{2+} (Mahmood et al. 2017). At low pH values, dissociation of the three-dimension structure of metal base exchanges, e.g. pectin hydrolyzed into its monomers, and thus resulting a low heavy metal biosorption (Khosravi et al. 2005). Nevertheless, low pH did not deteriorate the efficiency of heavy metal biosorption in the present study.

Influence of temperature

Table 1 shows the removal efficiency differences of each sample at 25±2 and 40°C. The differences in lead removal efficiency were calculated based on the subtraction of lead removal efficiency in treatment at 25±2 °C and the treatments at 40 °C. Positive values indicated heavy metal removal efficiency is greater, and vice versa. The magnitude of the value indicated the significance of temperature influences during the biosorption process. Generally, little effect of temperature was noticed on the lead removal between pH 4.5–5.5. However, biosorption performed at pH 6.0 showed consistent negative values regardless of bead types. The difference in biosorption efficiency (pH 6.0) at 40°C is slightly higher compared to 25±2 °C. Nonetheless, biosorption efficiency at pH 6.0 still lower compared to those treatments at pH 4.5 – 5.5 at both temperatures. This implies temperature has little effect on the biosorption. The finding is also in agreement with Sanyahumbi et al. (1998) and Antunes et al. (2001), the authors suggested that temperature (e.g.10-50 °C) had negligible effects on the gold(III) removal when *A. filiculoides* was used as biosorbent in their study. However, pH is the only factor that influenced gold(III) removal.

Likewise, several studies have suggested temperature has an insignificant effect on biosorption efficiency. For instance, pearl oyster mushroom, *Pleurotus ostreatus* displayed an insignificant change of biosorption behaviour at the temperature ranging from 20 – 45 °C. This presumably attributes to minor or

no changes on the biosorbent surface structure, and the chemistry of the groups involved in sequestering Pb(II) (Javaid et al. 2011). In contrast, a study suggested alginate-melamine hybrid sorbent (Li et al. 2018), and alginate-SBA-15 (nanoporous silica SBA-15) composite (Cheraghali et al. 2013) have higher lead biosorption ability with increasing temperature. This effect could be activated by a non-living biomass under regular temperatures. Increasing temperature could increase the rate of heavy metal diffusion within the internal pores of adsorbent particles. This largely owing to the lower viscosity of the solution, and the increasing desolvation of lead ions (Boudrahem et al. 2011; Srinivasa et al. 2013).

Biosorption kinetics

Nonlinear lines in the pseudo-first-order model graphs (Fig. 3) showed a coefficient of determination (R^2) values ranging of 0.4619 – 0.9912. On the other hand, linear lines in the pseudo-second-order model graphs (Fig. 4) showed R^2 values ranging of 0.9936 – 1.000. The pseudo-second-order kinetic model was selected to describe the biosorption kinetics, based on the R^2, which is closer to the unity (Boudrahem et al. 2011). This kinetic model indicates that biosorption process of Pb(II) was complex in CA, CA-UT, and CA-T beads, as more than one mechanism is involved. This model also signifies the surface biosorption involves chemisorption, which is a rate-limiting process due to physicochemical interactions between biosorbent and lead solution (Wang et al. 2007).

   The k_2 (rate constant), q_e (theoretical biosorption capacity at equilibrium), and h (initial biosorption rate) for each pH value, type of bead, and temperature were demonstrated in Table 2. It is important to note that the calculated q_e in all experiments is approximately 2 mg g^{-1}, in which metal uptake at equilibrium is 2 mg of Pb(II) per gram of biosorbent, regardless of temperature, pH, and type of biosorbents. Experimental qe was not examined here, due to longer experimental period is required to achieve its biosorption equilibrium time. It is also noted that initial biosorption rate (h), and rate constant (k_2) were highest at pH 4.5 and 5.0 in all treatment groups, this indicates biosorption capability of all beads (regardless of its type) was higher at pH 4.5 – 5.0 compared to pH 5.5 and 6.0. As mentioned early, pH is of particularly important in the determination of biosorption efficiency.

Table 1 The Pb(II) removal efficiency differences between 25 ± 2 °C and 40 °C at different pH

| Adsorbent	Time (Min)	Lead removal efficiency (%) differences			
		pH 4.5	pH 5.0	pH 5.5	pH 6.0
CA beads	60	0	-0.980	-1.627	-1.118
	120	-0.137	1.765	-0.765	-12.431
	180	0.235	1.961	3.039	-7.725
	240	0.157	1.627	-0.118	-1.843
	300	0.098	1.686	-0.353	0.196
	360	0.098	1.078	-0.196	0.529
CA-UT beads	60	1.549	-0.647	1.353	-1.216
	120	-0.294	1.961	4.216	-6.725
	180	1.510	3.196	6.314	-7.137
	240	1.922	3.039	2.471	-5.020
	300	1.216	2.686	0.529	-2.039
	360	1.157	2.000	0.941	-0.961
CA-T beads	60	1.588	-1.765	3.922	-3.176
	120	0.333	0.255	3.373	-13.471
	180	0.490	1.294	4.451	-11.314
	240	0.333	1.765	2.882	-12.745
	300	0	1.961	-0.333	-10.529
	360	0.059	0.745	-0.392	-7.941
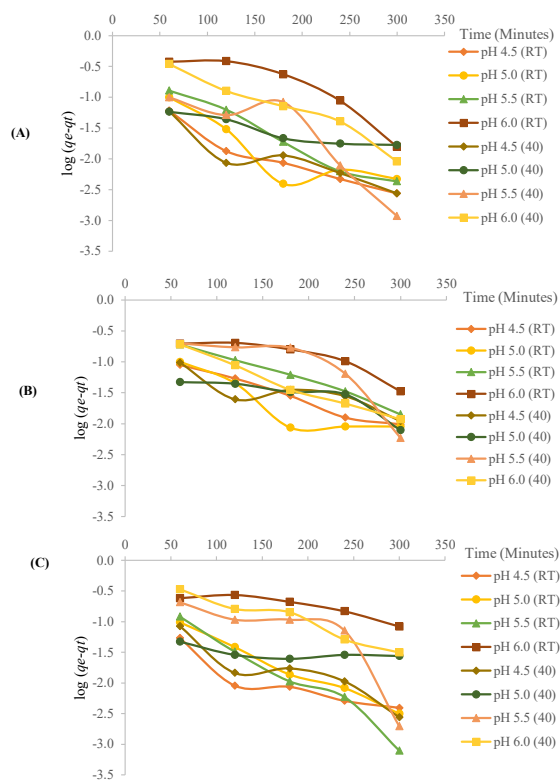
Fig. 3 Plot of pseudo-first-order linear equations for (A) CA beads, (B) CA-UT beads (C) CA-T beads for pH 4.5 – 6.0 at 25±2 ℃ (labelled as RT) and 40 ℃ (labelled as 40)
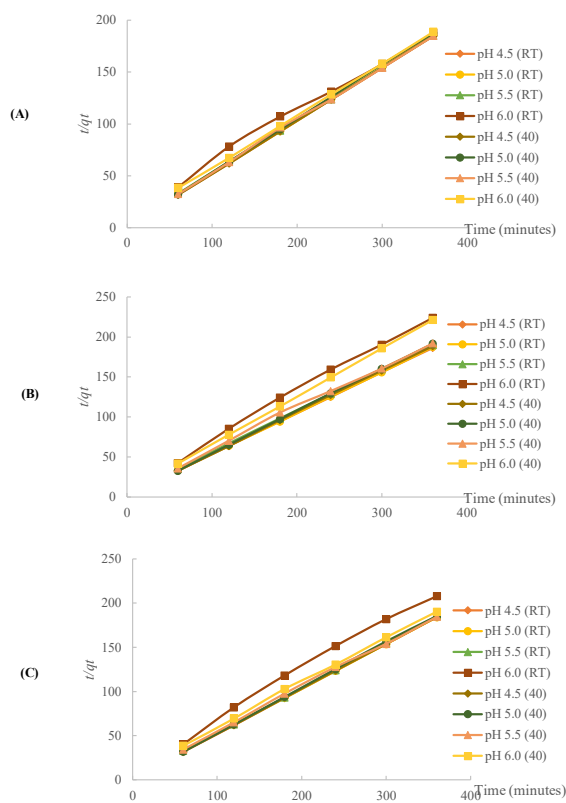

Fig. 4 Plot of pseudo-second-order linear equations for (A) CA beads, (B) CA-UT beads (C) CA-T beads for each pH at 25±2 ℃ (labelled as RT) and 40 ℃ (labelled as 40)

Intraparticle diffusion

In the intraparticle diffusion model, the diffusion-limited mechanism of Pb(II) biosorption was clearly observed in CA, CA-UT and CA-T, whereby q_t against $t^{1/2}$ values yield a straight line passes through the origin, this shows that biosorption process is controlled by intraparticle diffusion alone (Fig. 5). Nonetheless, if q_t against $t^{1/2}$ values generates multi-linear plot, it means several factors are influencing the biosorption process (Abdel-Ghani et al. 2015). In the present study, data indicated that the relationship between q_t and $t^{1/2}$ for all treatments was not directly proportionate to each other, as no single linear line was observed among the beads. This implies that several processes were affecting the biosorption process concurrently. This is also an evident to explain the biosorption process that was segregated into three stages in the present study. The deviation between the three stages may be due to the differences in the mass transfer rate in the initial, and final stages of biosorption (Tan and Hameed 2010). Based on the graph, three phases were observed, firstly, the initial sharp incline, which was the external surface, or boundary layer diffusion. The second incline is less steep, the intraparticle diffusion within the pores (a rate-limiting process). The third phase was attributed to the equilibrium state, at this point, intra-diffusion begins to occur at a lower rate due to low Pb(II) concentration in the solution.

In general, the present results showed three distinct phases; an initiative curve portion and followed by a linear portion and then a plateau in the graphs. The intraparticle diffusion constant, k_p1, k_p2, and k_p3 calculated from different group of beads (Table 3) showed that highest values were observed in k_p1, followed by k_p2, and lastly, k_p3. The intraparticle diffusion rate decreased along with time, however, the process was remained stable at the later stages.

Table 2 Pseudo-second-order kinetic parameters for the removal of Pb(II) by CA, CA-UT and CA-T beads in various pH and temperatures

Adsorbent	Temperature	pH	R^2	q_e Calculated (mg g^{-1})	K_2 (g mg^{-1} min)	h (mg g^{-1} min)
CA Beads	25±2 °C	4.5	1.000	1.959	0.273	1.048
		5.0	1.000	1.960	0.163	0.628
		5.5	1.000	1.976	0.098	0.381
		6.0	0.994	2.087	0.014	0.062
	40 °C	4.5	1.000	1.956	0.289	1.106
		5.0	0.999	1.930	0.178	0.663
		5.5	0.999	1.980	0.085	0.333
		6.0	0.999	1.992	0.032	0.128
CA-UT Beads	25±2 °C	4.5	1.000	1.953	0.122	0.467
		5.0	1.000	1.946	0.128	0.485
		5.5	0.999	1.941	0.053	0.201
		6.0	0.996	1.671	0.030	0.084
	40 °C	4.5	0.999	1.924	0.137	0.506
		5.0	0.999	1.891	0.159	0.568
		5.5	0.997	1.949	0.032	0.120
		6.0	1.000	1.671	0.061	0.171
CA-T Beads	25±2 °C	4.5	1.000	1.962	0.324	1.249
		5.0	1.000	1.978	0.141	0.550
		5.5	1.000	1.967	0.129	0.501
		6.0	0.993	1.795	0.023	0.075
	40 °C	4.5	1.000	1.967	0.188	0.728
		5.0	0.999	1.941	0.244	0.918
		5.5	0.999	2.005	0.043	0.172
		6.0	0.999	1.977	0.028	0.108

R^2 = coefficient of determination; q_e = quantity of Pb(II) adsorbed per unit weight of beads at equilibrium; k_2 = rate constant of pseudo-second-order; h = initial biosorption rate

Table 3 Intraparticle diffusion constant, k_p1, k_p2 and k_p3 for the removal of Pb(II) by CA, CA-UT and CA-T beads in various pH and temperatures

Adsorbent	Temperature	pH	k_p1	k_p2	k_p3
CA Beads	25±2°C	4.5	0.244	0.007	0.001
		5.0	0.238	0.012	0.002
		5.5	0.235	0.016	0.002
		6.0	0.199	0.039	0.010
	40 °C	4.5	0.244	0.006	0.002
		5.0	0.241	0.006	0.005
		5.5	0.239	0.009	0.002
		6.0	0.202	0.049	0.005
CA-UT Beads	25±2°C	4.5	0.238	0.010	0.004
		5.0	0.235	0.012	0.003
		5.5	0.220	0.020	0.009
		6.0	0.182	0.012	0.030
	40 °C	4.5	0.234	0.008	0.008
		5.0	0.237	0.002	0.008
		5.5	0.216	0.015	0.014
		6.0	0.185	0.023	0.006
CA-T Beads	25±2°C	4.5	0.245	0.014	0.001
		5.0	0.240	0.018	0.002
		5.5	0.235	0.028	0.002
		6.0	0.193	0.018	0.005
	40 °C	4.5	0.240	0.022	0.003
		5.0	0.245	0.006	0.004
		5.5	0.225	0.031	0.021
		6.0	0.201	0.031	0.019

k_p1 = intraparticle diffusion constant for the first slope; k_p2 = intraparticle diffusion constant for the second slope; k_p3 = intraparticle diffusion constant for the last slope

Biosorbent's functional group characterization

In the FTIR spectra analysis, the samples exhibited an absorption peak at around $3250 – 3290$ cm^{-1}, which is an evidence of O-H stretching (Fig. 6) The transmittance increased in the sequence of < CA < CA-UT and CA-T. This also indicates the encapsulation of *Azolla* with calcium alginates enforced the transmittance of O-H bonds. Samples also exhibited a weak absorption peak at around 2160 cm^{-1}, this attributable to C≡C stretching from the alkyne groups, whereby the transmittance of *Azolla* alone was higher than the alginate beads. Carboxylic groups stretching was split into asymmetric and symmetric C=O vibration. This can be observed in the regions of $1592 – 1614$ cm^{-1} and $1416 – 1420$ cm^{-1} respectively. The biosorption peaks at $1315 – 1360$ cm^{-1} were associated with the asymmetrical C=O stretching in the carboxylic groups, and aromatic C-O bonds.

FTIR spectra analysis is a powerful tool used to study biological molecules and characterize the functional groups on the adsorbent surface, it helps to explain the biosorption mechanism of the biosorbents (Aryal 2020). The increased biosorption uptake capacity exhibited by CA-T beads could be due to the high concentration of asymmetric and symmetric C=O vibrations observed in Figure 6. The increased concentration could be resulted by the chloride salts treatment applied to the *Azolla*. Preliminary Akali wash with pH 10.5 NaOH solution on *Azolla* removed protein groups that form a non-absorbable complex towards Pb^{2+} from the biosorbent' surface (Göksungur et al. 2003). Also, treatment with chloride solution mixture may increase the metal biosorption uptake, as the cations e.g. Mg^{2+}, Ca^{2+}, and Na^+, exchange with H^+ ions from (-COO)$_2$Mg, (-COO)$_2$Ca or (-COO)Na and the carboxyl group. These compounds act as the base for heavy metal ion exchange, and they are primary molecules involved in the heavy metal biosorption.

In conclusion, higher lead removal efficiency was noticed in CA-T beads, with an exception at pH 6.0. While CA-UT displayed the lowest performance in all tested parameters. The Pb(II) biosorption efficiency was increased from CA-UT < CA < CA-T. The present data showed that pre-treatment of *Azolla* with metal-chloride solutions slightly increased the lead biosorption efficiency, with an optimal level at pH ranging 4.5 - 5.0, regardless of temperatures. Kinetic models and FTIR analysis suggested that biosorption is a complex chemisorption process with multiple rate-limiting factors. The present data shows that immobilization

Azolla with alginate could enhance overall lead removal efficiency, and it could be a potential packing biomaterial in wastewater filter for heavy metal rehabilitation.
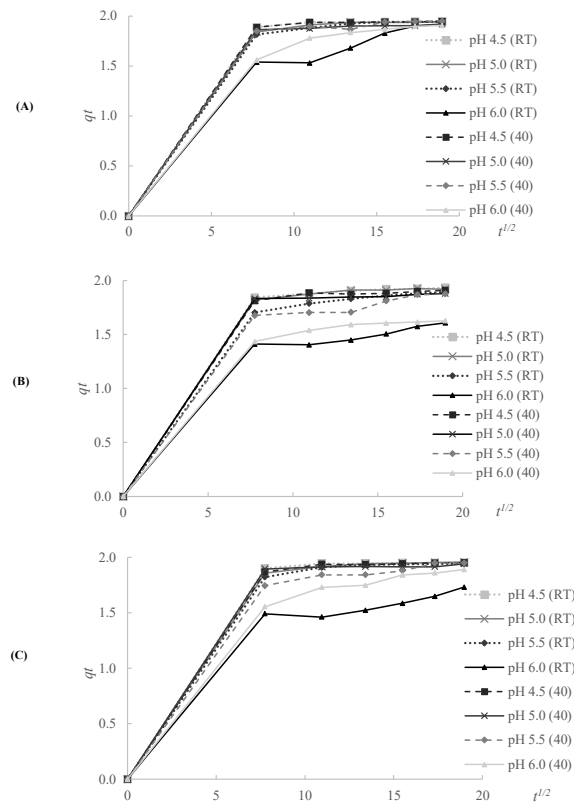

Fig. 5 Intraparticle diffusion model for Pb(II) biosorption by (A), CA beads (B) CA-UT beads and (C) CA-T beads at 25±2 °C (labelled as RT) and 40 °C (labelled as 40)
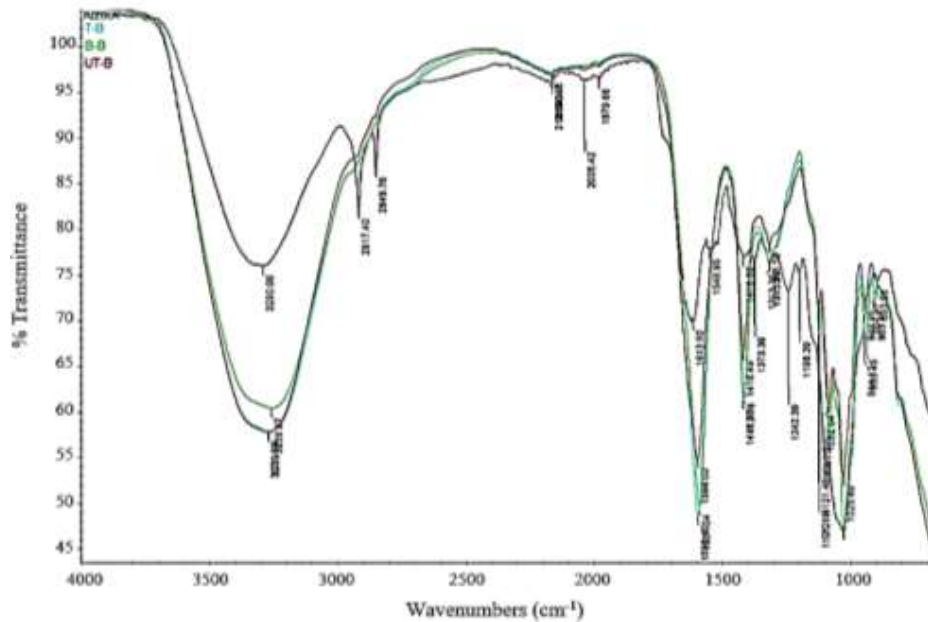

Fig. 6 FTIR spectra analysis of *Azolla*, CA, CA-UT and CA-T on the surface's functional groups

Future Recommendations

Future research should be emphasized on parameters e.g. biosorbent dosage, types of heavy metals, biosorbent surface's morphology (porosity of structure), and the reusability potential of the beads. More study needs to be carried out to elucidate the potential of alginate-immobilized *Azolla* at industrial scale.

References

Ab Razak N, Praveena S, Aris A, Hashim Z (2015) Drinking water studies: A review on heavy metal, application of biomarker and health risk assessment (a special focus in Malaysia). JEGH 5(4):297-310

Abdel-Ghani NT, Rawash ESA, El-Chaghaby GA (2015) Equilibrium and kinetic study for the adsorption of p-nitrophenol from wastewater using olive cake based activated carbon. Global J Environ Sci Manage 2(1):11-18

Ali H, Khan E, Ilahi I (2019) Environmental chemistry and ecotoxicology of hazardous heavy metals: Environmental persistence, toxicity, and bioaccumulation. J Chem, http://doi.org/10.1155/2019/6730305

Antunes A, Watkins G, Duncan J (2001) Batch studies on the removal of gold(III) from aqueous solution by *Azolla filiculoides*. Biotechnol Lett 23(4):249-251

Aryal M (2020) A comprehensive study on the bacterial biosorption of heavy metals: materials, performances, mechanisms, and mathematical modelling. Rev Chem Eng. http://doi.org/10.1515/revce-2019-0016

Boudrahem F, Aissani-Benissad F, Soualah A (2011) Adsorption of lead(II) from aqueous solution by using leaves of date trees as an adsorbent. J Chem Eng Data 56(5):1804-1812

Cheraghali R, Tavakoli H, Sepehrian H (2013) Preparation, characterization and lead sorption performance of alginate-SBA-15 composite as a novel adsorbent. Sci Iran 20(3):1028–1034

Cohen-Shoel N, Barkay Z, Ilzycer D, Gilath I, Tel-Or E (2002) Biofiltration of toxic elements by *Azolla* biomass. Water Air Soil Poll 135:93-104

Fiol N, Poch J, Villaescusa I (2005) Grape stalks wastes encapsulated in calcium alginate beads for Cr(VI) removal from aqueous solutions. Sep Sci Technol 40(5):1013-1028

Fu F, Wang Q (2011) Removal of heavy metal ions from wastewaters: a review. J Environ Manage 92(3):407-418

Gebremedhin K, Berhanu T (2015) Determination of some selected heavy metals in fish and water samples from Hawassa and Ziway lakes. Sci J Analytic Chem 3(1): 10-16

Göksungur Y, Űren S, Gűvenç U (2003) Biosorption of copper ions by caustic treated waste baker's yeast biomass. Tr J Biol 27:23–29

Hlaing CS, Kyu KK, Win T (2011) Removal of some toxic heavy metals by means of adsorption onto biosorbent composite (Coconut shell charcoal - calcium alginate) beads. Univ Res J 4(3):237–251

Ho YS, McKay G (2000) The kinetics of sorption of divalent metal ions onto sphagnum moss peat. Water Res 34:735–742

Hossain MA (2013) Development of novel biosorbents in removing heavy metals from aqueous solution. Thesis (PhD, Environmental Engineering) University of Technology (UTS) Sydney

Javaid A, Bajwa R, Shafique U, Anwar J (2011) Removal of heavy metals by adsorption on *Pleurotus ostreatus*. Biomass Bioenerg 35(5):1675-1682

Jeyakumar R, Chandrasekaran V (2014) Adsorption of lead (II) ions by activated carbons prepared from marine green algae: equilibrium and kinetics studies. Int J Ind Chem 5(1):1-9

Kanamarlapudi SLRK, Chintalpudi VK, Muddada S (2018) Application of biosorption for removal of heavy metals from wastewater. Biosorption, Jan Derco and Branislav Vrana, IntechOpen, http://doi.org/10.5772/intechopen.77315.

Kariuki Z, Kiptoo J, Onyancha D (2017) Biosorption studies of lead and copper using rogers mushroom biomass '*Lepiota hystrix*'. S Afr J Chem Eng 23:62-70

Khosravi M, Rakhshaee R, Ganji M (2005) Pre-treatment processes of to remove Pb(II), Cd(II), Ni(II) and Zn(II) from aqueous solution in the batch and fixed-bed reactors. J Hazard Mater 127(1-3):228-237

Lagergren S (1898) About the theory of so called adsorption of soluble substances. Kungliga Svenska Vetenskapsakad. Handl 24:1–39

Li K, Wu G, Wang M, Zhou X, Wang Z (2018) Efficient removal of lead ions from water by a low-cost alginate-melamine hybrid sorbent. Appl Sci 8(9):1518

Mahmood Z, Amin A, Zafar U, Raza M, Hafeez I, Akram A (2017) Adsorption studies of cadmium ions on alginate–calcium carbonate composite beads. Appl Water Sci 7(2):915-921

Mashkani SG, Ghazvini PTM (2009) Biotechnological potential of *Azolla filiculoides* for biosorption of Cs and Sr: Application of micro-PIXE for measurement of biosorption. Bioresour Technol 6:1915-1921

Mathew BB, Jaishankar M, George V, Beeregowda KN (2016) Role of bioadsorbents in reducing toxic metals. J Toxicol 2016:1–13

Muzzarelli RAA, Tanfani F, Scarpini G (1980) Chelating, film Forming, and coagulating ability of the chitosan-glucan complex from *Aspergillus niger* industrial wastes, Biotechnol Bioeng 22:885-896

Naga Babu A, Krishna Mohan G, Kalpana K, Ravindhranath K (2017) Removal of lead from water using calcium alginate beads

doped with hydrazine sulphate-activated red mud as adsorbent. J Anal Methods Chem 2017:1-13

Quiton KG, Doma B Jr, Futalan CM, Wan M-W (2018) Removal of chromium(VI) and zinc(II) from aqueous solution using kaolin-supported bacterial biofilms of Gram-negative *E. coli* and Gram-positive *Staphylococcus epidermidis*. Sustain Environ Res 28:206–213

Rahman MS, Sathasivam KV (2015) Heavy metal adsorption onto *Kappaphycus* sp. from aqueous solutions: The use of error functions for validation of isotherm and kinetics models. Biomed Res Int 2015:1–13

Raize O, Argaman Y, Yannai S (2002). Mechanisms of biosorption of different heavy metals by brown marine macroalgae. Biotechnol Bioeng 87(4):451-458

Salman A, Ayatolla N, Naser J (2012) Potential of *Azolla filiculoides* in the removal of Ni and Cu from wastewaters. Afr J Biotechnol 11(95):16158-16164

Salman HA, Ismail IM, Mostafa TM, Sulaymon AH (2014) Biosorption of heavy metals: A review. J Chem Technol Biot 3(4):74-102

Sanyahumbi D, Duncan J, Zhao M, Hille R (1998) Removal of lead from solution by the non-viable biomass of the water fern *Azolla filiculoides.* Biotechnol Lett 20(8):745-747

Sharma B, Singh S, Siddiqi N (2014) Biomedical implications of heavy metals induced imbalances in redox systems. Biomed Res Int. http://doi.org/10.1155/2014/640754

Sood A, Uniyal PL, Prasanna R, Ahluwalia AS (2012) Phytoremediation potential of aquatic macrophyte, *Azolla*. Ambio 41(2):122–137

Srinivasa Rao J, Kesava Rao C, Prabhakar G (2013) Optimization of biosorption performance of Casuarina leaf powder for the removal of lead using central composite design. J Environ Anal Toxicol 3:166. http://doi.org/10.4172/2161-0525.1000166

Taghi ganji M, Khosravi M, Rakhshaee R (2005) Biosorption of Pb, Cd, Cu and Zn from the wastewater by treated *Azolla filiculoides* with $H_2O_2/MgCl_2$. Int J Environ Sci Technol 1(4):265-271

Tan I, Hameed B (2010) Adsorption isotherms, kinetics, thermodynamics and desorption studies of basic dye on activated carbon derived from oil palm empty fruit bunch. J Appl Sci Res 10(21):2565-2571

Tseveendorj E, Enkhdul T, Lin S, Dorj D, Oyungerel Sh, Soyol-Erdene TO (2018) Biosorption of lead (II) from an aqueous solution using biosorbents prepared from water plants. Mong J Chem 18(44):52-61

Uysal Y, Taner F (2009) Effect of pH, temperature, and lead concentration on the bioremoval of lead from water using *Lemna minor*. Int J Phytoremediation 11(7):591-608

Wang H, Zhou A, Peng F, Yu H, Yang J (2007) Mechanism study on adsorption of acidified multi-walled carbon nanotubes to Pb(II). J. Colloid Interface Sci 316:277–283

Wei W, Wang Q, Li A, Yang J, Ma F, Pi S, Wu D (2016) Biosorption of Pb (II) from aqueous solution by extracellular polymeric substances extracted from *Klebsiella* sp. J1: Adsorption behavior and mechanism assessment. Sci Rep 6:31575. http://doi.org/10.1038/srep31575

Zhao LL, Wang J, Zhang PP, Gu QQ, Gao CC (2018) Absorption of heavy metal ions by alginate. *In:* Bioactive seaweeds for food applications. http://doi.org/10.1016/ B978-0-12-813312-5.00013-3

Publisher's Note
IAU remains neutral with regard to jurisdictional claims in published maps and institutional affiliations.